Chiral Self-sorting Process with Ditopic Ligands: Alternate- or Block-Metallopolymer Assembly as Function of the Metal Ion

Maya Marinova,[§] Maria Torres-Werlé,[§] Grégory Taupier,[§] Aline Maisse-François,[§] Thierry Achard,[§]

Alex Boeglin,[§] Kokou Dodzi (Honorat) Dorkenoo,[§] Stéphane Bellemin-Laponnaz[*,§]*

§ IPCMS (Institut de Physique et Chimie des Matériaux de Strasbourg), CNRS-Université de

Strasbourg, 23 rue du Loess BP 43, F-67034 Strasbourg, France

E-mail: bellemin@unistra.fr
http://www.ipcms.unistra.fr/

Supporting Information

1. **General remarks** S2

2. **Generic procedure for the synthesis of monotopic & ditopic VinylBox** S3

3. **Titration experiments of *rac* DivinylBox with copper metal salt** S6

4. **CD titration experiments of (S) DivinylBox with zinc metal salt** S7

5. **Circular Dichroism of enantiopure DivinylBox metallopolymer** S8

6. **^{1}H NMR- and ^{13}C NMR spectra of all novel compounds** S9

7. **Density Functional Theory (DFT) and time dependent (TD) DFT calculations** S11

8. **X-ray tables of DivinylBox ligand** S15

9. **References** S24

1 General remarks

Solvents were purified and degassed by standard procedures. All reagents were used without further purification. MeOH was purchased with Aldrich without any purification. Pyridine employed during complexation reactions was distilled from calcium hydride and carefully stored under argon. ^{1}H and ^{13}C NMR spectra were recorded by using a Bruker Avance 300 spectrometer using the residual solvent peak as a reference ($CDCl_3$: δ H= 7.26 ppm; δ C= 77.16 ppm) at 298 K. Positive mode electrospray ionization mass spectra (ESI-MS) were recorded on microTOF, Bruker Daltonics. X-Ray diffraction studies were carried out by Dr. Lydia Brelot at Institut de Chimie X-ray Facility of the University of Strasbourg. Crystal data were collected at 173 K using a MoKα graphite monochromated (λ = 0.71073 Å) radiation on a Nonius KappaCCD diffractometer. The structures were solved using direct methods with SHELXS97552 and refined against F2 using the SHELXL97 software.553 Non-hydrogen atoms were refined anisotropically. Hydrogen atoms were generated according to stereochemistry and refined using a riding model in SHELXL97.

Density Functional Theory (DFT) and time dependent (TD-) DFT calculations have been performed with the Gaussian 09 software using the hybrid B3-LYP functional and the polarizable continuum model for methanol at a qualitative level of accuracy in order to assess possible ligand conformations and how they are affected by metal chelation, to identify the optical transitions of interest and to gauge their optical activity.

2 Generic procedure for the synthesis of monotopic & ditopic VinylBox

2.1 2.1 Synthesis of DiVinylBox:

N,N'-bis[(1*S*)-1-isopropyl-2-hydroxyethyl]malonide (1)
Dimethylmalonate (38.18 mmol, 4.4 mL) and (*S*)-Valinol (77.5 mmol, 8 g) were put in a Schlenk. Then, and under argon, a catalytic amount of NaH was added. The mixture was stirred overnight at 140°C. The next day, MeOH is evaporated under vacuo. The yellowish solid was then dissolved in a minimum of dichloromethane and precipitated with ether. A white powder was obtained (29 mmol, 7.9g, 76%). ^{1}H NMR (300 MHz, DMSO-d_6): δ = 7.73 (d, ^{3}J= 9.2 Hz, 2H; -N*H*), 4.60 (bs, 2H; -C*H*NH), 3.60-3.52 (m, 4H; CH_2OH), 3.10 (s, 2H; -CH_2CO), 1.84-1.73 (m, 2H; -C*H*(CH_3)$_2$), 0.82 (dd, ^{3}J= 6.8 Hz, ^{4}J= 2.4 Hz, 12 H; -C*H*(CH_3)$_2$).

N,N'-bis[(1*S*)-1-isopropyl-2-chloro]malonide (2)
Compound **1** (29 mmol, 7.924 g) was dissolved in toluene (250 mL) and stirred for 10 min. A light yellow solution was obtained. Then, SOCl2 (63.8 mL, 4.6 mL) was added dropwise. The resulting mixture was stirred and heated for 4h at 90 °C. After this time, the mixture was left to cool down at r.t and poured onto an ice cold 20% KOH solution. Then, it was extracted with dichloromethane (3x150 mL) and the organic phase washed with NaHCO3. The solution was dried over Na2SO4 and reduced under pressure. A yellow/orange solid was obtained (26.2 mmol, 8.2 g, 90%). ^{1}H NMR (300 MHz, $CDCl_3$): δ = 6.98 (d, ^{3}J= 8.7 Hz, 2H; -N*H*), 4.01-3.94 (m, 2H; -C*H*NH), 3.72-3.66 (m, 4H; CH_2OH), 3.27 (s, 2H; -CH_2CO), 2.02-1.94 (m, 2H; -C*H*(CH_3)$_2$), 0.96 (dd, ^{3}J= 6.8 Hz, 4J= 1.5 Hz, 12 H; -C*H*(CH_3)$_2$).

1,1-bis[(4*S*)-4-isopropyl-4,5-dihydrooxazol-2-yl]methane (*S,S*)-Box [1]
To compound **2** obtained (26.2 mmol, 8.152 g) was added KOH (65.5 mmol, 3.675 g) and the whole was dissolved in MeOH (250 mL). The orange solution was heated at reflux for 3h. Then, it was let to cool down at r.t and the mixture was poured onto water (260 mL), extracted with dichloromethane (3x130 mL), washed with brine, dried over Na2SO4 and reduced under pressure. An orange oil was obtained and then, distilled under vacuo to afford a yellow crystalline solid (15 mmol, 3.4 g, 57%). $_{1}$H NMR (300 MHz, $CDCl_3$): δ = 4.26 (t, ^{3}J= 7.7 Hz, 2H; -C*H*NC), 4.03-3.92 (m, 4H; -CH_2OC), 3.34 (s, 2H; -CH_2), 1.80-1.73 (m, 2H; -C*H*(CH_3)$_2$), 0.91 (d, ^{3}J= 6.8 Hz, 12 H; -C*H*(CH_3)$_2$); ^{13}C{1H} NMR (300 MHz, $CDCl_3$): δ =161.5 (-N*C*O), 72.2 (-*C*HN), 70.5 (-*C*H_2O), 32.3 (-*C*H(CH_3)$_2$), 28.3 (-*C*H_2), 18.6, 17.9 (-CH(*C*H_3)$_2$);MS (ESI +): *m/z* (%): 239.17 [M+H]+; elemental analysis calcd (%) for C13H22N2O2 (238.33): C 65.51, H 9.30, N11.75; found C 62.06, H 8.95, N 11.26.

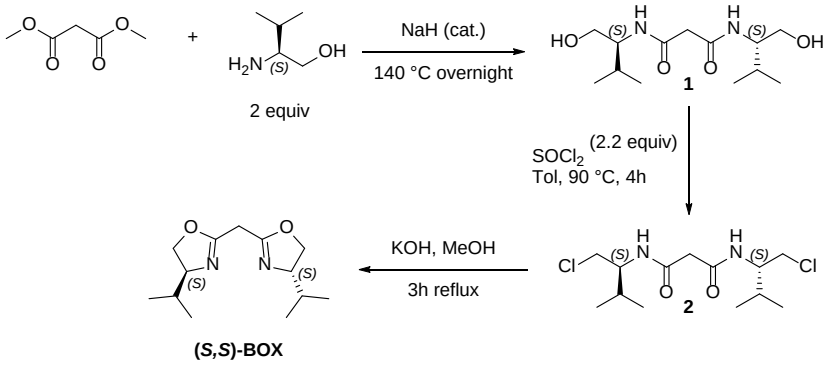

Figure S1. Synthesis of bisoxazoline unit (*S,S*)-Box.

Synthesis of 1,4-bis(2,2-bis((S)-4-isopropyl-4,5-dihydrooxazol-2-yl)vinyl)benzene (*S,S,S,S*)- DiVinylBox

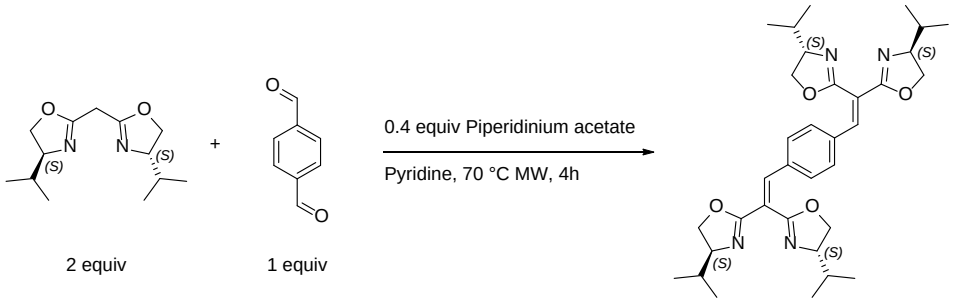

Figure S2. Synthesis of DiVinylBox ligands through Knoevenagel condensation

Thermic conditions:
1,1-bis[(4S)-4-isopropyl-4,5-dihydrooxazol-2-yl]methane (0.84 mmol, 200 mg), piperidinium acetate (0.17 mmol, 24.22 mg) and terephtaldehyde (0.42 mmol, 56.33 mg) were put together in a Schlenk. Pyridine (3 mL) was added and the mixture was heated and stirred at 65 °C for 72h. After this time, the solvent was evaporated trap to trap. The resulting yellow-orange solid was purified by silica gel column chromatography (AcOEt/MeOH, 95:5) yielding a white solid (0.30 mmol, 174.8 mg, 71%).

Microwave assisted conditions:
1,1-bis[(4S)-4-isopropyl-4,5-dihydrooxazol-2-yl]methane (0.839 mmol, 200 mg, 2 equiv), 1,4-Phthalaldehyde (0.461 mmol, 62 mg, 1.1 equiv) and freshly made piperidinium acetate (0.168 mmol, 24 mg) were suspended in dry pyridine (4 mL). The mixture was then stirred for 2 min before being subjected to microwave irradiation for 4 hours at 70 °C. After cooling to r.t., the pyridine was removed under vacuum giving a yellow oil, which was purified by silica-gel column chromatography (AcOEt/MeOH, 95:5) to yield a white solid (150 mg, 62%). $[\alpha]_D^{20}$ =- 154 $cm^3g^{-1}dm^{-1}$ (*c* = 0.02 in MeOH); ^{1}H NMR (300 MHz, $CDCl_3$) δ 7.53 (s, 2H), 7.44 (s, 4H), 4.28-4.41(m, C*H*-N, 4H), 4.19-3.96 (m, CH_2-O, 8H), 1.74-1.89 (m, C*H*$(CH_3)_2$, 4H), 1.07-0.77 (m, 6 x CH_3, 24H). ^{13}C NMR (101 MHz, $CDCl_3$) δ = 161.8 (2 x N=*C*O), 160.4 (2 x N=*C*O), 139.9 (2 x H*C*=C), 135.4 (2 x C_{Ar}), 129.6 (4 x *C*H$_{Ar}$), 120.0 (2 x *C*=CH), 73.1 (2 x N*C*H), 73.1 (2 x N*C*H), 70.6 (2 x OCH_2), 70.4 (2 x OCH_2), 33.1(2 x *C*H$(CH_3)_2$), 32.6 (2 x *C*H$(CH_3)_2$), 19.2, 18.9, 18.7 and 18.4 (8 x *C*H_3). IR (KBr): $\tilde{\nu}$ = 1674 cm-1 (s, C=N); MS (ESI +): *m/z*= 239.18 $[C_{13}H_{22}N_2O_2+H]^+$, 327.19 $[C_{20}H_{26}N_2O_2+H]^+$, 597.34 $[M+Na]^+$, 813.52 $[M+C_{13}H_{22}N_2O_2+H]^+$; elemental analysis calcd (%) for $C_{34}H_{46}N_4O_4$ (574.75): C 71.05, H 8.07, N 9.75; found C 70.78, H 8.11, N 9.48.

2.2 Synthesis of VinylBox:

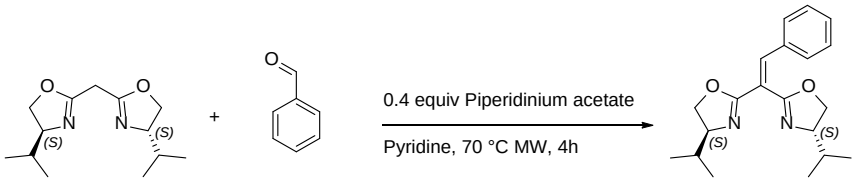

Figure S3. Synthesis of DiVinylBox ligands through Knoevenagel condensation

Synthesis of (*S,S*)-VinylBOX

Using the same procedure depicted for ditopic ligand. 1,1-bis[(4S)-4-isopropyl-4,5-dihydrooxazol-2-yl]methane (0.839 mmol, 200 mg, 1 equiv), freshly distilled benzaldehyde (0.461 mmol, 62 mg, 1 equiv) and freshly made piperidinium acetate (0.168 mmol, 24 mg, 5 equiv) were suspended in dry pyridine (4 mL). The mixture was then stirred for 2 min before being subjected to microwave irradiation for 4 hours at 70 °C. After cooling to r.t., the pyridine was removed under vacuum giving yellow oil. The crude material was taken up on DCM, washed with a $NaHCO_3$, dry with Na_2SO_4 and concentrate under vacuum. The yellow oil was purified by silica-gel column chromatography deactivated by small amount of trimethylamine (first pure DCM and then pure AcOEt) to yield a white soft-solid (192 mg, 70 %). $[\alpha]_D^{20} =$- 12,46 $cm^3g^{-1}dm^{-1}$ (*c* = 0.35 in $CHCl_3$); ^{1}H NMR (300 MHz,$CDCl_3$): δ 7.57 (s, 1H, ArHC=C), 7.46–7.49 (m, 2H, H_{Ar}), 7.32–7.34 (m, 3H, H_{Ar}), 4.29–4.39 (m, 2H, CH), 4.04–4.17 (m, 4H, CH_2), 1.73–1.88 (m, 2H, $CH(CH_3)_2$), 0.99 (s, 3H, $CH(CH_3)_2$), 0.97 (s, 3H, $CH(CH_3)_2$), 0.94 (s, 3H, $CH(CH_3)_2$), 0.89 (s, 3H, $CH(CH_3)_2$) ppm. ^{13}C NMR (75 MHz, $CDCl_3$): δ 161.8, 160.4, 140.8, 134.2, 129.43, 129.35, 128.35, 119.0, 72.87, 72.85, 70.23, 70.16, 32.88, 32.36, 18.93, 18.75, 18.43 and 18.21 ppm.
These data are in agreement with the one reported in literature. [2]

3 Titration experiments of *rac* DivinylBox with copper metal salt

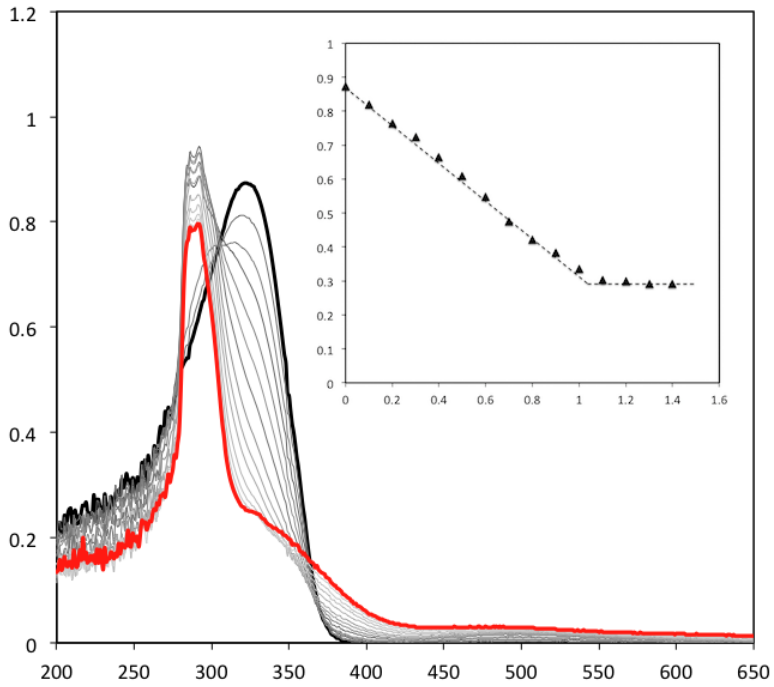

Figure S4. Titration of racemic DivinylBox ligand concentration of 2.5 10^{-5} M in MeOH with $Cu(BF_4)_2$ followed by UV-vis spectroscopy. The spectra corresponding to 0 and 1 eq. of Cu^{2+} added are displayed as black and red trace, respectively. Black arrow indicates the variation of the spectra features upon addition of the salt. The insets show the change in absorbance at 328 nm as a function of added Cu^{2+}.

4 CD titration experiments of (S) DivinylBox with zinc metal salt

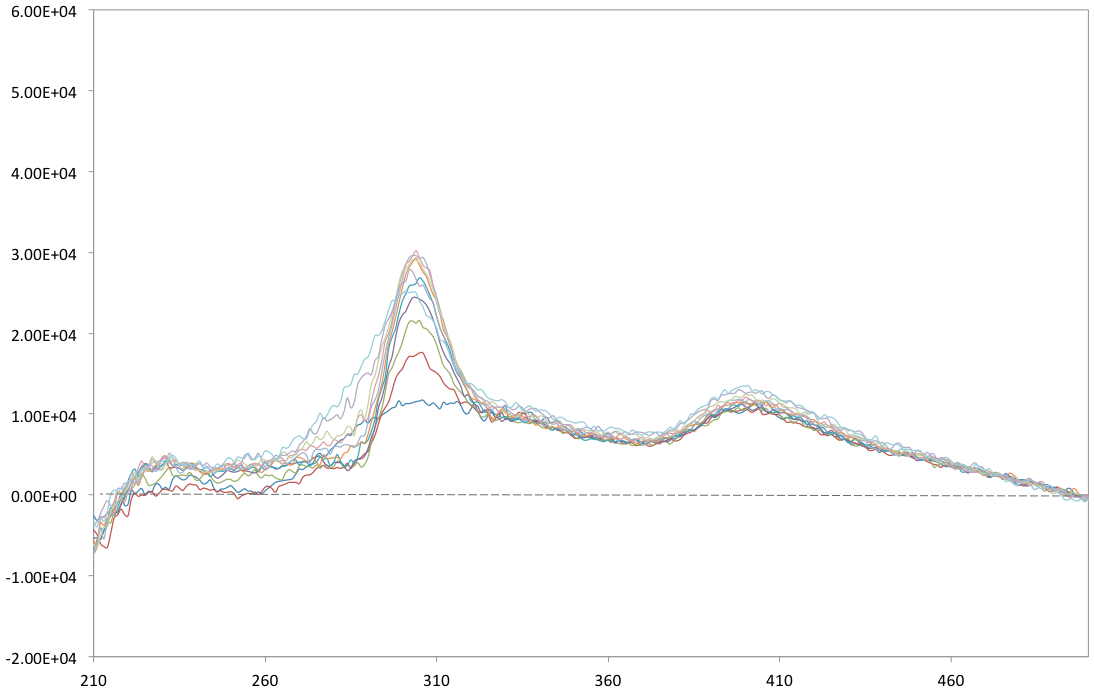

Figure S5. CD spectral changes in the titration of (S) DivinylBox solution (MeOH, c=5×10^{-5} M) with $Zn(BF_4)_2$: 0 equiv. (blue line, *bottom*) to 2 equiv. of zinc ion (orange line, *top*).

5 Circular Dichroism of enantiopure DivinylBox metallopolymer

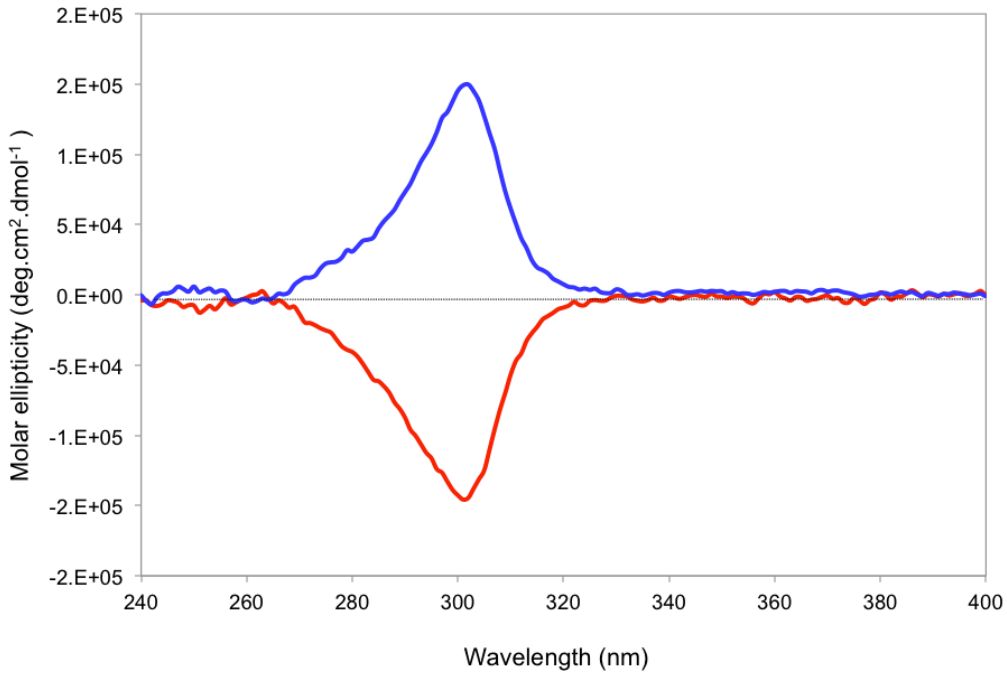

Figure S6. Mirror image of the CD spectra of enantiopure metallopolymers generated from $Cu(BF_4)_2$ and (S) and (R) DiVinylBox; [Cu] = 2.5 10^{-5} M (blue and red lines, respectively) (solvent: MeOH).

6 ^{1}H NMR AND ^{13}C-NMR SPECTRA OF ALL NOVEL COMPOUNDS

(*S*,*S*,*S*,*S*)-DiVinylBOX

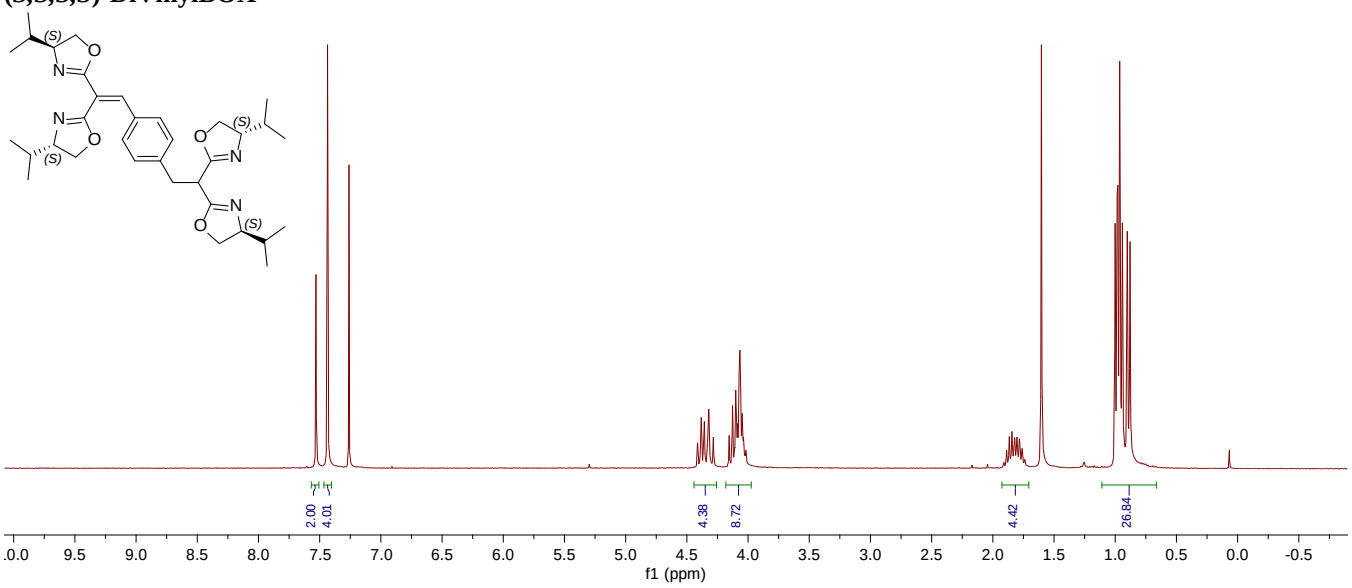

Figure S7. ^{1}H NMR (300 MHz) $CDCl_3$

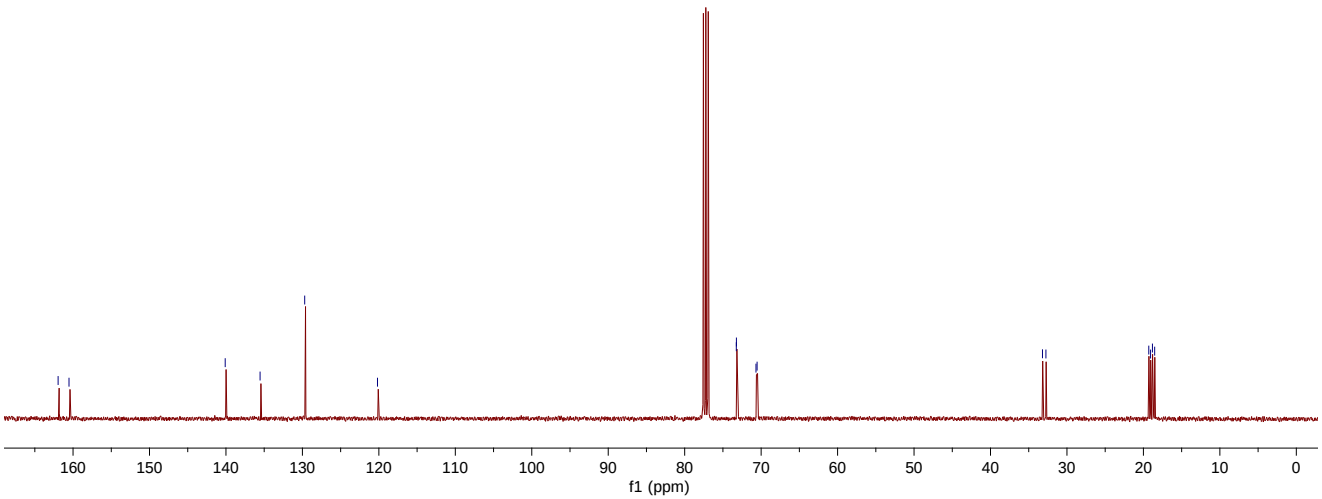

Figure S8. ^{13}C NMR (126 MHz) $CDCl_3$

(*S*,*S*)-VinylBOX

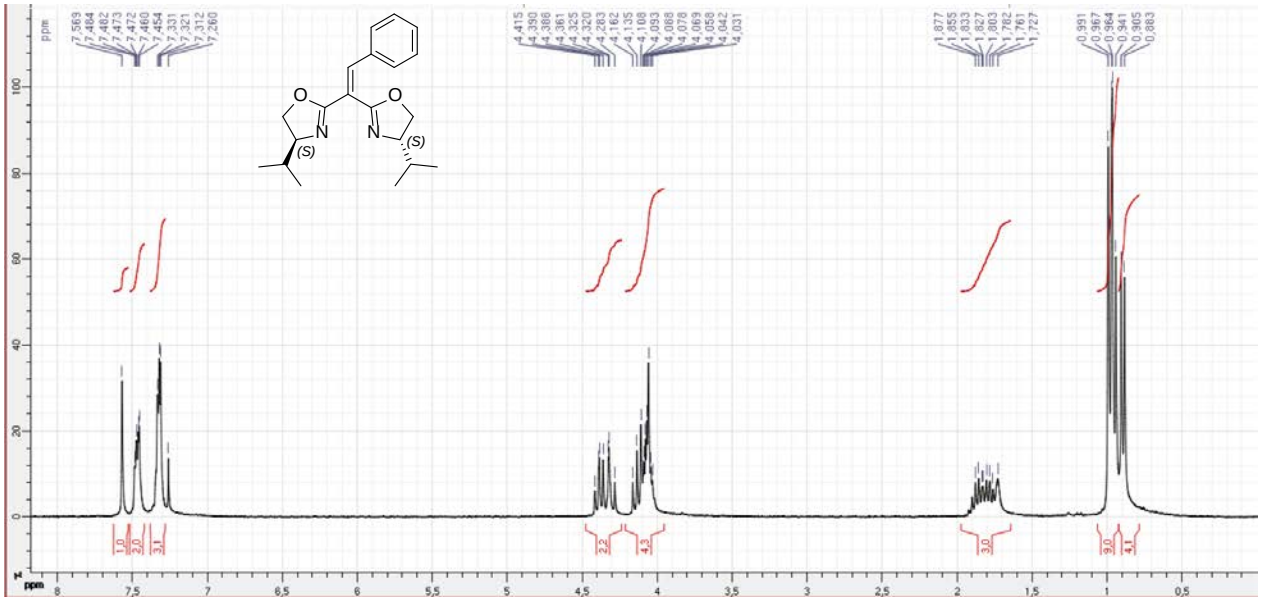

Figure S9. ^{1}H NMR (300 MHz) $CDCl_3$

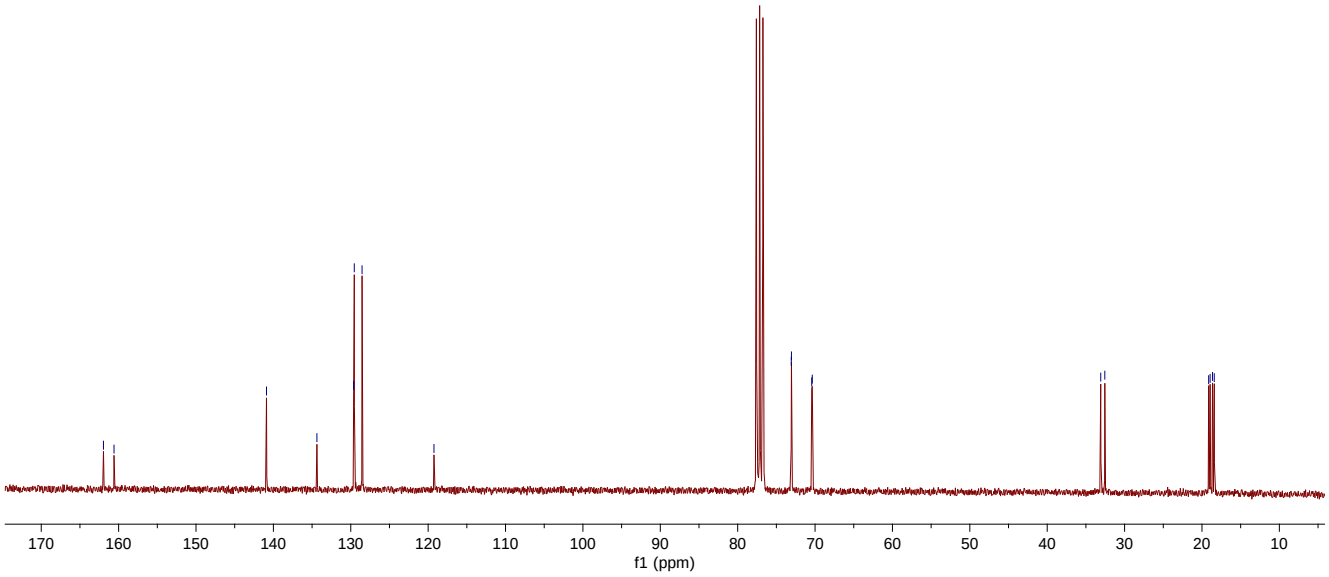

Figure S10. ^{13}C NMR (126 MHz) $CDCl_3$

7 Density Functional Theory (DFT) and time dependent (TD) DFT calculations

DFT geometries of the free DiVinylBox ditopic ligand and of its bimetallic complexes with copper and zinc have been optimized using the hybrid B3-LYP functional along with the 6-31G(d,p) basis set while using the polarizable continuum model (PCM) for methanol as implemented in the Gaussian 09 software .[3] The TD-DFT calculations have been run either at the same level of precision or, in the case of the free ligand, also with the larger 6-311+G(d,p) basis set to gauge the level of basis set dependency of the resulting excited states (the convergence of 32 roots has routinely been asked for, except for the *syn+* form of the Cu complex for which it has also been pushed to 48 roots but the results showed no significant changes).

7.1 Free DiVinylBox ligand in solution in methanol:

Even when not taking into consideration all the possible orientations of the isopropyl steric groups, DFT geometry optimizations of the free ligand converge to several conformational structures differing in the positioning of the two non-conjugated oxazolines with respect to their nearest phenyl hydrogen atom. On either end, the heterocyclic atom closest to a phenyl H atom may be the oxygen or the nitrogen. That these conformations are indeed stable has been tested by running normal mode calculations where the lowest frequencies have always been found to be positive.
The conformation shown below is the one that resembles the X-ray crystal structure the most: it combines the two situations mentioned above for the positioning of the out-of-plane oxazolines. For this set of orientations of the isopropyl groups with respect to their oxazoline rings it is also the configuration with the lowest DFT+PCM energy. The one aspect were X-ray and DFT structures differ is in the exact orientation of the out-of-plane five membered rings which are held orthogonally to the phenyl plane in the crystal while the calculated geometries allow for some departure from orthogonality.

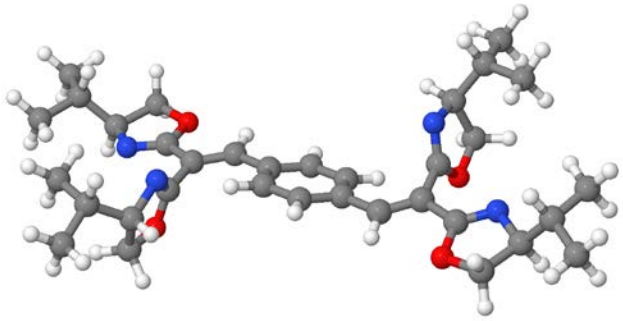

Figure S11. The stable DFT geometry of DiVinylBox most similar to the conformation adopted in the crystal.

TD-DFT (B3-LYP, 6-32G(d,p)) results for the transitions to the first excited singlet states for the above geometry are summarized in the following table.

	6-31G(d,p)			6-311+G(d,p)		
	wavelength (nm)	oscillator strength	rotary strength (cgs)	wavelength (nm)	oscillator strength	rotary strength (cgs)
S1 ← S0	360.6	1.6380	-65.80	365.5	1.6400	-68.66
S2 ← S0	328.7	0.0117	-0.78	328.8	0.0096	-2.05
S3 ← S0	327.5	0.0194	2.69	327.1	0.0152	2.35
S4 ← S0	309.4	0.0009	1.90	310.1	0.0017	4.12
S5 ← S0	294.6	0.0198	1.34	298.1	0.0182	2.03
S6 ← S0	287.6	0.0715	27.26	288.8	0.0538	23.42

Table S1. TD-DFT results (B3-LYP).

The rotary strengths indicated are given in units of 10^{-40} erg.esu.cm/Gauss. The marked blue shift and the width of the experimental absorption band as well as the absence of detectable levels of circular dichroism for free ligands in methanol together with the possibility to find several stable geometries in the DFT calculations are indications that the DiVinylBox

compound is a highly labile entity in solution, at least as far as the librations of the individual oxazolines as well as those of the head groups as a whole are concerned.

7.2 Bimetallic complex of Cu(II) with a DiVinylBox and MeOH ligands:

Geometries for a fully coordinated ditopic ligand have been obtained with two Cu(II) ions by completing their coordination spheres with methanol molecules. To allow for the proper left-right correlation of the odd d-electron on the copper atoms, calculations for the Cu(II) bimetallic complex have been carried out by running the calculations in the unrestricted scheme and asking for a triplet multiplicity both for the ground (DFT geometry optimization) and for the excited states (TD-DFT optical transitions).

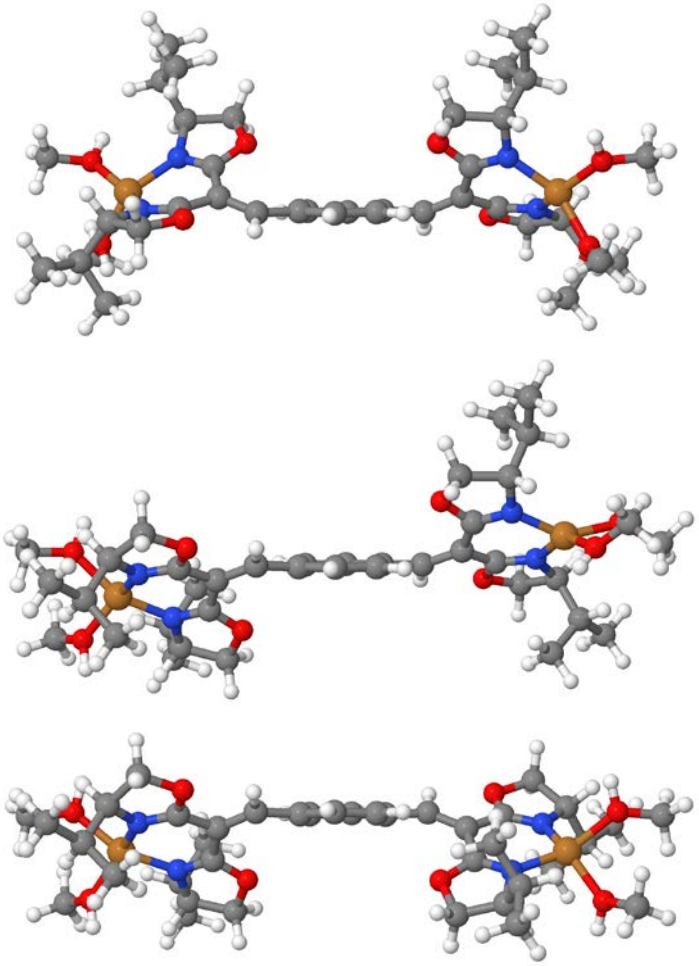

Figure S12. Three conformations of the bimetallic copper complex. Top: *boat* with positive optical activity (OA), middle: *chair* with low negative OA, and bottom: *boat* with negative OA.

The total energy of formation of the copper complex in its first *boat* conformation above is computed at E = -5586.3491856 Ha. This makes it more stable by 1.26 kJ/mol than the *chair* configuration which is computed at E = -5586.3487068 Ha. The second *boat* conformation has a total energy of E = -5586.3490559 Ha, only 0.34 kJ/mol above that of the first *boat* structure and 0.92 kJ/mol below that of the *chair* geometry. The fully allowed ligand centered optical transition is obtained as the 14th or the 16th root of the TD-DFT calculations and while contributions of excitations out of methanol centered orbitals are found in the lower energy transitions, including the #11 root which happens also to be of LMCT character, the optical transitions of interest turn out to be largely uncontaminated by such contributions and is a DiVinylBox centered π-π* transition.

Cu(II) complex form	Excited state #	wavelength (nm)	oscillator strength	rotary power (cgs)
Boat+	(root #11)	468.65	0.1273	-90.94
	(root #14)	410.33	1.2882	248.66
	(root #16)	407.00	0.1849	70.91
Chair	(root #16)	404.01	1.3723	35.12
Boat-	(root #11)	473.05	0.2022	-182.66
	(root #16)	403.02	1.2893	-258.29

Table S2. Calculated wavelength and rotary power for Cu complexes.

As opposed to what is seen in experiment, the main absorption is red shifted upon complexation with metal ions in the DFT calculations. This can be attributed to the enlargement of the pi electron system not compensated by the resulting increase in dihedral angle of the vinyl groups with respect to the phenyl plane in the optimal geometries. Of course, allowance must also be made for the coordination spheres which poorly reproduce the real situation. The rotary powers obtained illustrate the fact that the *chair* form gives rise to a pseudo inversion center for the π-electron system which is located in the center of the phenyl ring while the *boat* conformations result in a pseudo helical axis corresponding to the phenyl's six-fold symmetry axis. The detection of a positive CD in titration experiments indicates that entropic factors must dominate over internal energies for the links in the polymer strands to mostly adopt the *boat+* conformation.

7.3 Bimetallic complex of Zn(II) with a DiVinylBox and MeOH ligands:

Again, the geometries for a fully coordinated ditopic ligand have been obtained with two Zn(II) ions by completing their coordination spheres with methanol molecules. Because of the full d shell, all calculations have been performed for a closed shell singlet. The first *boat* conformation shown below is computed to have a total energy of formation of E = -5864.0923684 Ha, the *chair* configuration to have E = -5864.0945766 Ha (i.e. lower by 5.8 kJ/mol) and the second *boat* geometry to have E = -5864.0956603 Ha (lower again by 2.8 kJ/mol). Although such small energy differences may be compensated by entropic factors, it is of interest to note that, in contrast to the previous complexes, the first *boat* conformation is not favored here by the energetics obtained at the DFT level with the PCM solvation model for methanol. It may be of interest to mention that running the same DFT and TD-DFT calculations without the use of the solvation model leads to little changes in transition energies but noticeable increases in oscillator strengths as well as decreases in rotary strengths showing that the possible stable conformations of the complex are more strongly bent out of conjugation when the interaction of the local atomic net charges and polarities are allowed to interact with a polarizable dielectric environment.

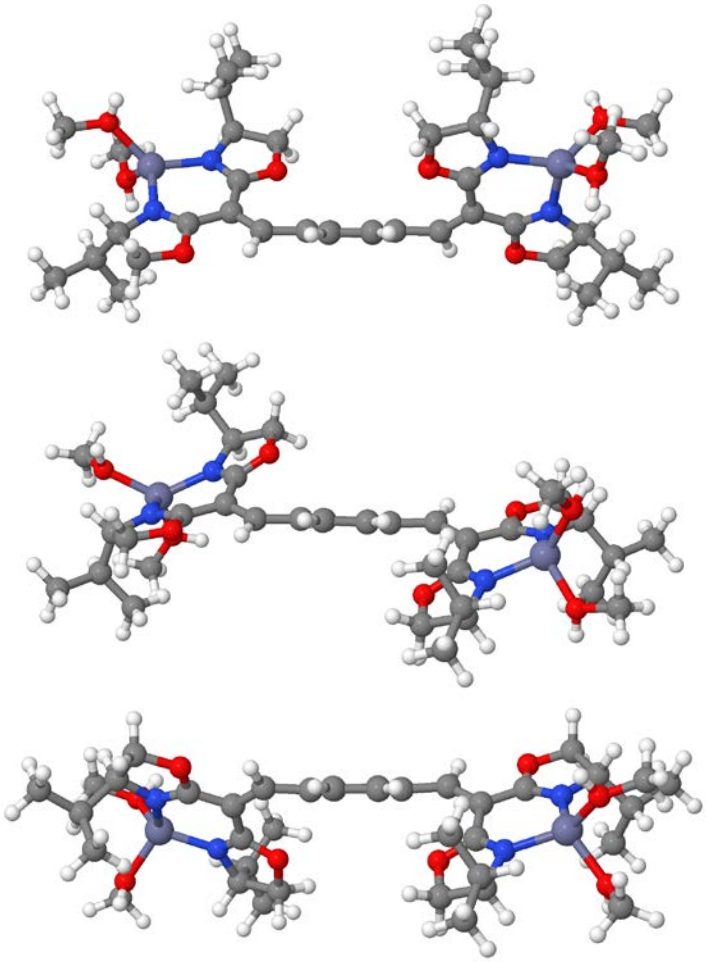

Figure S13. Three conformations of the bimetallic zinc complex. Top: *syn* with positive optical activity (OA), middle: *anti* with low negative OA, and bottom: *syn* with negative OA.

The fully allowed ligand centered optical transition corresponds to the first singlet transition obtained in TD-DFT and it is chiefly of ($\pi^* \leftarrow \pi$, DiVinylBox centered) HOMO-LUMO type:

Zn(II) complex form	Wavelength (nm)	oscillator strength	rotary strength (cgs)
Syn+	404.17	1.4232	299.71
Anti	395.57	1.4706	-69.76
Syn-	398.78	1.3946	-410.43

Table S3. Calculated wavelength and rotary power for Zn complexes.

8 X-ray tables of DivinylBOX ligand

Single crystals of **(*S,S,S,S*)-DiVinylBOX** were grown in chloroform. The crystals were placed in oil, and a colourless plate single crystal of dimensions 0.40 x 0.25 x 0.15 mm was selected, mounted on a glass fibre and placed in a low-temperature N_2 stream.

X-Ray diffraction data collection was carried out on a Bruker APEX II DUO Kappa-CCD diffractometer equipped with an Oxford Cryosystem liquid N_2 device, using Cu-Kα radiation (λ = 1.54178 Å). The crystal-detector distance was 40mm. The cell parameters were determined (APEX2 software) [4] from reflections taken from three sets of 20 frames, each at 10s exposure. The structure was solved by Direct methods using the program SHELXS-2013 [5]. The refinement and all further calculations were carried out using SHELXL-2013 [3]. The H-atoms were included in calculated positions and treated as riding atoms using SHELXL default parameters. The non-H atoms were refined anisotropically, using weighted full-matrix least-squares on F^2. A semi-empirical absorption correction was applied using SADABS in APEX2 [6]; transmission factors: T_{min}/T_{max} = 0.6699/0.7528. The methyl group C28 is disordered over two positions with a 0.6/0.4 ratio. The H-atom H26 is also disordered over two positions with the same ratio.

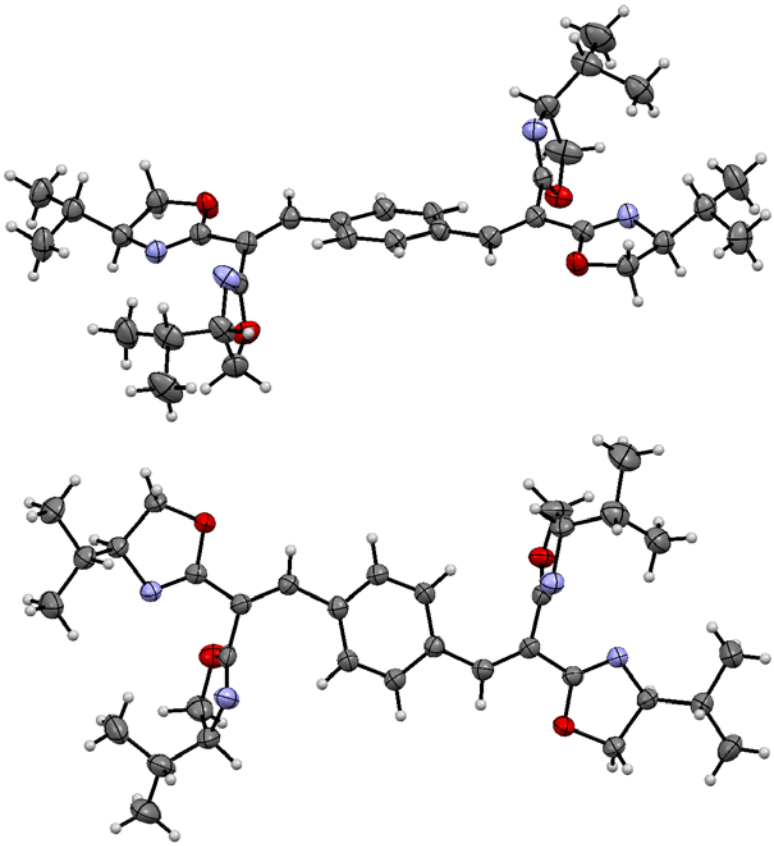

Figure S14. Ortep views of **(*S,S,S,S*)-DiVinylBOX** ligand X-ray structure.

Table S4. Crystal data and structure refinement for sblta160205	
Identification	sblta160205
Empirical formula	C_{34} H_{46} N_4 O_4
Formula weight	574.75
Temperature	173(2)K
Wavelength	1.54178 A
Crystal system	Triclinic
space group	*P 1*
Unit cell dimensions	
a (Å)	5.4629(2)
b (Å)	10.0985(3)
c (Å)	15.3132(5)
α (°)	90.204(2)
β (°)	96.2270(10)
γ (°)	103.0290(10)
Volume ($Å^3$)	817.838
Z	1
Calculated density (Mg/m^3)	1.167
Absorption coefficient (mm^{-1})	0.611
F(000)	310
Crystal size (mm)	0.400 x 0.250 x 0.150
Theta range (°)	4.496 to 66.908
Limiting indices	-6<=h<=4, -12<=k<=11, -18<=l<=18
Reflections collected / unique / R_{int}	12957 / 4089 / 0.0269
Completeness to theta	67.679; 97.0 %
Absorption Correction	Semi-empirical from equivalents
Max. and min. transmission	0.7528 and 0.6699
Refinement method	Full-matric least-square on F^2
Data / restraints / parameters	4089 / 3 / 391
Goodness-of-fit on F_2	1.048

Final R indices *R1, wR2 (I>2σ(I))*	0.0363; 0.0950
R1, wR2 (all data)	0.0382; 0.0969
Absolute structure parameter	-0.04(12)
Largest diff. peak and hole (e.Å^{-3})	0.212; -0.169
Extinction coefficient	n/a

Table S5. Bond lengths [Å]

C1-C2	1.398(4)	C19-H19A	0.979
C1-C6	1.394(4)	C19-H19B	0.980
C1-C7	1.471(3)	C19-H19C	0.981
C2-H2	0.950	C20-H20A	0.981
C2-C3	1.382(4)	C20-H20B	0.980
C3-H3	0.950	C20-H20C	0.980
C3-C4	1.402(4)	C21-H21	0.950
C4-C5	1.400(4)	C21-C22	1.344(4)
C4-C21	1.469(3)	C22-C23	1.487(3)
C5-H5	0.950	C22-C29	1.466(3)
C5-C6	1.385(4)	C23-N3	1.263(3)
C6-H6	0.950	C23-O3	1.353(4)
C7-H7	0.950	C24-H24A	0.990
C7-C8	1.342(4)	C24-H24B	0.990
C8-C9	1.466(3)	C24-C25	1.512(5)
C8-C15	1.485(3)	C24-O3	1.447(3)
C9-N1	1.265(3)	C25-H25	1.000
C9-O1	1.359(3)	C25-C26	1.527(4)
C10-H10A	0.990	C25-N3	1.483(4)
C10-H10B	0.991	C26-H26	0.999
C10-C11	1.540(4)	C26-C27	1.524(5)
C10-O1	1.443(3)	C26-C28	1.610(7)
C11-H11	1.000	C27-H27A	0.980
C11-C12	1.523(4)	C27-H27B	0.980
C11-N1	1.470(3)	C27-H27C	0.980
C12-H12	0.999	C28-H28A	0.980
C12-C13	1.521(4)	C28-H28B	0.980
C12-C14	1.521(4)	C28-H28C	0.980
C13-H13A	0.979	C29-N4	1.272(3)

C13-H13B	0.980	C29-O4	1.356(3)
C13-H13C	0.981	C30-H30A	0.990
C14-H14A	0.981	C30-H30B	0.990
C14-H14B	0.980	C30-C31	1.523(4)
C14-H14C	0.980	C30-O4	1.456(3)
C15-N2	1.251(4)	C31-H31	0.999
C15-O2	1.368(3)	C31-C32	1.525(4)
C16-H16A	0.991	C31-N4	1.486(3)
C16-H16B	0.990	C32-H32	1.000
C16-C17	1.534(5)	C32-C33	1.531(4)
C16-O2	1.441(4)	C32-C34	1.510(4)
C17-H17	1.000	C33-H33A	0.981
C17-C18	1.526(5)	C33-H33B	0.979
C17-N2	1.478(4)	C33-H33C	0.980
C18-H18	1.000	C34-H34A	0.980
C18-C19	1.529(4)	C34-H34B	0.980
C18-C20	1.515(5)	C34-H34C	0.980

Table S6. Angles [deg]

C2-C1-C6	118.0(2)	C18-C20-H20B	109.5
C2-C1-C7	117.7(2)	C18-C20-H20C	109.4
C6-C1-C7	124.3(2)	H20A-C20-H20B	109.5
C1-C2-H2	119.1	H20A-C20-H20C	109.5
C1-C2-C3	121.7(3)	H20B-C20-H20C	109.6
H2-C2-C3	119.1	C4-C21-H21	115.6
C2-C3-H3	119.8	C4-C21-C22	128.8(2)
C2-C3-C4	120.3(2)	H21-C21-C22	115.6
H3-C3-C4	119.8	C21-C22-C23	124.1(2)
C3-C4-C5	117.8(2)	C21-C22-C29	120.9(2)
C3-C4-C21	123.8(2)	C23-C22-C29	115.1(2)
C5-C4-C21	118.4(2)	C22-C23-N3	125.0(2)
C4-C5-H5	119.2	C22-C23-O3	115.6(2)
C4-C5-C6	121.6(3)	N3-C23-O3	119.4(2)
H5-C5-C6	119.2	H24A-C24-H24B	108.8
C1-C6-C5	120.4(3)	H24A-C24-C25	110.7
C1-C6-H6	119.8	H24A-C24-O3	110.8
C5-C6-H6	119.8	H24B-C24-C25	110.7
C1-C7-H7	115.1	H24B-C24-O3	110.7
C1-C7-C8	129.6(2)	C25-C24-O3	105.2(3)
H7-C7-C8	115.2	C24-C25-H25	108.5
C7-C8-C9	121.0(2)	C24-C25-C26	115.3(3)
C7-C8-C15	125.5(2)	C24-C25-N3	104.4(2)
C9-C8-C15	113.5(2)	H25-C25-C26	108.5

C8-C9-N1	125.0(2)	H25-C25-N3	108.5
C8-C9-O1	116.1(2)	C26-C25-N3	111.4(3)
N1-C9-O1	118.9(2)	C25-C26-H26	109.9
H10A-C10-H10B	108.9	C25-C26-C27	111.3(3)
H10A-C10-C11	110.8	C25C26C28	107.1(3)
H10A-C10-O1	110.8	H26-C26-C27	109.9
H10B-C10-C11	110.8	H26-C26-C28	109.9
H10B-C10-O1	110.8	C27-C26-C28	108.8(3)
C11-C10-O1	104.6(2)	C26-C27-H27A	109.5
C10-C11-H11	108.6	C26-C27-H27B	109.5
C10-C11-C12	114.1(2)	C26-C27-H27C	109.5
C10-C11-N1	103.9(2)	H27A-C27-H27B	109.5
H11-C11-C12	108.6	H27A-C27-H27C	109.5
H11-C11-N1	108.6	H27B-C27-H27C	109.4
C12-C11-N1	112.9(2)	C26-C28-H28A	109.5
C11-C12-H12	108.2	C26-C28-H28B	109.4
C11-C12-C13	109.7(2)	C26-C28-H28C	109.5
C11-C12-C14	111.1(2)	H28A-C28-H28B	109.5
H12-C12-C13	108.2	H28A-C28-H28C	109.5
H12-C12-C14	108.2	H28B-C28-H28C	109.4
C13-C12-C14	111.3(3)	C22-C29-N4	124.7(2)
C12-C13-H13A	109.5	C22-C29-O4	116.4(2)
C12-C13-H13B	109.5	N4-C29-O4	118.8(2)
C12-C13-H13C	109.4	H30A-C30-H30B	109.0
H13A-C13-H13B	109.5	H30A-C30-C31	111.0
H13A-C13-H13C	109.5	30A-C30-O4	111.0
H13B-C13-H13C	109.4	H30B-C30-C31	111.0
C12-C14-H14A	109.5	H30B-C30-O4	111.0
C12-C14-H14B	109.5	C31-C30-O4	103.8(2)
C12-C14-H14C	109.5	C30-C31-H31	108.3
H14A-C14-H14B	109.4	C30-C31-C32	114.3(2)
H14A-C14-H14C	109.4	C30-C31-N4	103.9(2)
H14B-C14-H14C	109.5	H31-C31-C32	108.4
C8-C15-N2	127.6(2)	H31-C31-N4	108.4
C8-C15-O2	113.4(2)	C32-C31-N4	113.4(2)
N2-C15-O2	119.0(2)	C31-C32-H32	108.2
H16A-C16-H16B	108.8	C31-C32-C33	109.7(2)
H16A-C16-C17	110.8	C31-C32-C34	111.1(2)
H16A-C16-O2	110.7	H32-C32-C33	108.2
H16B-C16-C17	110.8	H32-C32-C34	108.2
H16B-C16-O2	110.8	C33-C32-C34	111.3(3)
C17-C16-O2	104.9(2)	C32-C33-H33A	109.5
C16-C17-H17	108.9	C32-C33-H33B	109.5
C16-C17-C18	115.6(3)	C32-C33-H33C	109.5

C16-C17-N2	103.8(2)	H33A-C33-H33B	109.4
H17-C17-C18	108.9	H33A-C33-H33C	109.5
H17-C17-N2	108.9	H33B-C33-H33C	109.5
C18-C17-N2	110.6(3)	C32-C34-H34A	109.5
C17-C18-H18	107.7	C32-C34-H34B	109.5
C17-C18-C19	110.9(3)	C32-C34-H34C	109.5
C17-C18-C20	112.0(3)	H34A-C34-H34B	109.5
H18-C18-C19	107.7	H34A-C34-H34C	109.4
H18-C18-C20	107.7	H34B-C34-H34C	109.5
C19-C18-C20	110.7(3)	C9-N1-C11	106.9(2)
C18-C19-H19A	109.5	C15-N2-C17	107.1(2)
C18-C19-H19B	109.5	C23-N3-C25	106.0(2)
C18-C19-H19C	109.4	C29-N4-C31	105.9(2)
H19A-C19-H19B	109.5	C9-O1-C10	105.4(2)
H19A-C19-H19C	109.5	C15-O2-C16	105.2(2)
H19B-C19-H19C	109.5	C23-O3-C24	105.0(2)
C18-C20-H20A	109.4	C29-O4-C30	104.8(2)

Table S7. Torsion angles [deg]

C6C1C2H2	-177.0	C17C18C19H19C	-60.4
C6C1C2C3	2.9(4)	H18C18C19H19A	62.0
C7C1C2H2	2.9	H18C18C19H19B	-58.0
C7C1C2C3	-177.1(2)	H18C18C19H19C	-178.0
C2C1C6C5	-2.6(4)	C20C18C19H19A	-55.5
C2C1C6H6	177.5	C20C18C19H19B	-175.5
C7C1C6C5	177.4(2)	C20C18C19H19C	64.5
C7C1C6H6	-2.5	C17C18C20H20A	-46.5
C2C1C7H7	-27.1	C17C18C20H20B	-166.5
C2C1C7C8	152.8(3)	C17C18C20H20C	73.4
C6C1C7H7	152.8	H18C18C20H20A	71.7
C6C1C7C8	-27.2(4)	H18C18C20H20B	-48.3
C1C2C3H3	177.8	H18C18C20H20C	-168.4
C1C2C3C4	-2.2(4)	C19C18C20H20A	-170.9
H2C2C3H3	-2.2	C19C18C20H20B	69.2
H2C2C3C4	177.8	C19C18C20H20C	-50.9
C2C3C4C5	1.0(4)	C4C21C22C23	5.0(4)
C2C3C4C21	178.6(3)	C4C21C22C29	-176.1(2)
H3C3C4C5	-179.0	H21C21C22C23	-175.0

H3C3C4C21	-1.4	H21C21C22C29	3.8
C3C4C5H5	179.3	C21C22C23N3	81.2(4)
C3C4C5C6	-0.7(4)	C21C22C23O3	-97.9(3)
C21C4C5H5	1.6	C29C22C23N3	-97.8(3)
C21C4C5C6	-178.4(3)	C29C22C23O3	83.2(3)
C3C4C21H21	-157.1	C21C22C29N4	175.3(3)
C3C4C21C22	22.8(4)	C21C22C29O4	-3.7(4)
C5C4C21H21	20.4	C23C22C29N4	-5.7(4)
C5C4C21C22	-159.7(3)	C23C22C29O4	175.2(2)
C4C5C6C1	1.6(4)	C22C23N3C25	179.4(2)
C4C5C6H6	-178.5	O3C23N3C25	-1.5(3)
H5C5C6C1	-178.4	C22C23O3C24	-178.7(2)
H5C5C6H6	1.5	N3C23O3C24	2.2(3)
C1C7C8C9	-178.7(2)	H24AC24C25H25	5.1
C1C7C8C15	-1.8(4)	H24AC24C25C26	-116.8
H7C7C8C9	1.3	H24AC24C25N3	120.6
H7C7C8C15	178.2	H24BC24C25H25	125.8
C7C8C9N1	-171.3(2)	H24BC24C25C26	3.9
C7C8C9O1	9.5(3)	H24BC24C25N3	-118.6
C15C8C9N1	11.5(4)	O3C24C25H25	-114.6
C15C8C9O1	-167.8(2)	O3C24C25C26	123.5(3)
C7C8C15N2	87.3(4)	O3C24C25N3	1.0(3)
C7C8C15O2	-93.7(3)	H24AC24O3C23	-121.4
C9C8C15N2	-95.6(3)	H24BC24O3C23	117.8
C9C8C15O2	83.4(3)	C25C24O3C23	-1.7(3)
C8C9N1C11	-177.1(2)	C24C25C26H26	-173.9
O1C9N1C11	2.1(3)	C24C25C26C27	64.2(4)
C8C9O1C10	-178.9(2)	C24C25C26C28	-54.6(4)
N1C9O1C10	1.8(3)	H25C25C26H26	64.2
H10AC10C11H11	9.8	H25C25C26C27	-57.7
H10AC10C11C12	-111.5	H25C25C26C28	-176.5
H10AC10C11N1	125.2	N3C25C26H26	-55.2
H10BC10C11H11	130.8	N3C25C26C27	-177.1(3)
H10BC10C11C12	9.5	N3C25C26C28	64.2(4)
H10BC10C11N1	-113.8	C24C25N3C23	0.2(3)
O1C10C11H11	-109.7	H25C25N3C23	115.7
O1C10C11C12	129.0(2)	C26C25N3C23	-124.9(3)
O1C10C11N1	5.7(3)	C25C26C27H27A	60.8

H10AC10O1C9	-124.1	C25C26C27H27B	-59.3
H10BC10O1C9	114.9	C25C26C27H27C	-179.1
C11C10O1C9	-4.6(3)	H26C26C27H27A	-61.1
C10C11C12H12	-57.3	H26C26C27H27B	178.9
C10C11C12C13	60.6(3)	H26C26C27H27C	59.0
C10C11C12C14	-175.9(2)	C28C26C27H27A	178.5
H11C11C12H12	-178.5	C28C26C27H27B	58.5
H11C11C12C13	-60.6	C28C26C27H27C	-61.4
H11C11C12C14	62.9	C25C26C28H28A	-51.6
N1C11C12H12	61.0	C25C26C28H28B	-171.5
N1C11C12C13	178.9(2)	C25C26C28H28C	68.5
N1C11C12C14	-57.6(3)	H26C26C28H28A	67.7
C10C11N1C9	-4.8(3)	H26C26C28H28B	-52.2
H11C11N1C9	110.6	H26C26C28H28C	-172.2
C12C11N1C9	-128.9(2)	C27C26C28H28A	-171.9
C11C12C13H13A	-58.6	C27C26C28H28B	68.1
C11C12C13H13B	-178.7	C27C26C28H28C	-51.9
C11C12C13H13C	61.4	C22C29N4C31	-176.9(2)
H12C12C13H13A	59.2	O4C29N4C31	2.1(3)
H12C12C13H13B	-60.8	C22C29O4C30	-172.0(2)
H12C12C13H13C	179.3	N4C29O4C30	8.9(3)
C14C12C13H13A	178.0	H30AC30C31H31	20.5
C14C12C13H13B	58.0	H30AC30C31C32	-100.4
C14C12C13H13C	-61.9	H30AC30C31N4	135.6
C11C12C14H14A	-60.1	H30BC30C31H31	141.9
C11C12C14H14B	179.9	H30BC30C31C32	21.0
C11C12C14H14C	59.9	H30BC30C31N4	-103.0
H12C12C14H14A	-178.8	O4C30C31H31	-98.7
H12C12C14H14B	61.2	O4C30C31C32	140.4(2)
H12C12C14H14C	-58.8	O4C30C31N4	16.3(3)
C13C12C14H14A	62.4	H30AC30O4C29	-134.4
C13C12C14H14B	-57.6	H30BC30O4C29	104.2
C13C12C14H14C	-177.6	C31C30O4C29	-15.2(3)
C8C15N2C17	177.4(2)	C30C31C32H32	-56.4
O2C15N2C17	-1.6(3)	C30C31C32C33	61.4(3)
C8C15O2C16	-177.5(2)	C30C31C32C34	-175.1(3)
N2C15O2C16	1.6(3)	H31C31C32H32	-177.3
H16AC16C17H17	3.7	H31C31C32C33	-59.4

H16AC16C17C18	-119.2	H31C31C32C34	64.1
H16AC16C17N2	119.5	N4C31C32H32	62.4
H16BC16C17H17	124.6	N4C31C32C33	-179.8(2)
H16BC16C17C18	1.7	N4C31C32C34	-56.3(3)
H16BC16C17N2	-119.6	C30C31N4C29	-11.7(3)
O2C16C17H17	-115.8	H31C31N4C29	103.3
O2C16C17C18	121.3(3)	C32C31N4C29	-136.3(2)
O2C16C17N2	0.0(3)	C31C32C33H33A	62.9
H16AC16O2C15	-120.3	C31C32C33H33B	-57.0
H16BC16O2C15	118.9	C31C32C33H33C	-177.1
C17C16O2C15	-0.8(3)	H32C32C33H33A	-179.2
C16C17C18H18	-173.4	H32C32C33H33B	60.8
C16C17C18C19	69.0(4)	H32C32C33H33C	-59.2
C16C17C18C20	-55.2(4)	C34C32C33H33A	-60.5
H17C17C18H18	63.7	C34C32C33H33B	179.6
H17C17C18C19	-53.9	C34C32C33H33C	59.5
H17C17C18C20	-178.1	C31C32C34H34A	176.4
N2C17C18H18	-55.9	C31C32C34H34B	56.3
N2C17C18C19	-173.4(3)	C31C32C34H34C	-63.7
N2C17C18C20	62.3(4)	H32C32C34H34A	57.7
C16C17N2C15	0.8(3)	H32C32C34H34B	-62.4
H17C17N2C15	116.7	H32C32C34H34C	177.6
C18C17N2C15	-123.7(3)	C33C32C34H34A	-61.1
C17C18C19H19A	179.5	C33C32C34H34B	178.9
C17C18C19H19B	59.5	C33C32C34H34C	58.9

9 References

(1) Campbell, C. D.; Concellon, C.; Smith, A. D. Catalytic enantioselective Steglich rearrangements using chiral N-heterocyclic carbenes. *Tetrahedron: Asymmetry*, **2011**, *22*, 797-811.

(2) Burke, A.J.; Carreiro, E.P.; Chercheja, S.; Moura, N.M.M.; Ramalho, J.P.; Rorigues, A.I.; Santos, C.I.M. Cu(I) catalysed cycl opropanation of olefins: Stereoselectivity studies with Arylid-Box and Isbut-Box ligands. *J. Organomet. Chem.* **2007**, *692*, 4863–4874.

(3) Gaussian 09, Revision D.01, M. J. Frisch, G. W. Trucks, H. B. Schlegel, G. E. Scuseria, M. A. Robb, J. R. Cheeseman, G. Scalmani, V. Barone, B. Mennucci, G. A. Petersson, H. Nakatsuji, M. Caricato, X. Li, H. P. Hratchian, A. F. Izmaylov, J. Bloino, G. Zheng, J. L. Sonnenberg, M. Hada, M. Ehara, K. Toyota, R. Fukuda, J. Hasegawa, M. Ishida, T. Nakajima, Y. Honda, O. Kitao, H. Nakai, T. Vreven, J. A. Montgomery, Jr., J. E. Peralta, F. Ogliaro, M. Bearpark, J. J. Heyd, E. Brothers, K. N. Kudin, V. N. Staroverov, T. Keith, R. Kobayashi, J. Normand, K. Raghavachari, A. Rendell, J. C. Burant, S. S. Iyengar, J. Tomasi, M. Cossi, N. Rega, J. M. Millam, M. Klene, J. E. Knox, J. B. Cross, V. Bakken, C. Adamo, J. Jaramillo, R. Gomperts, R. E. Stratmann, O. Yazyev, A. J. Austin, R. Cammi, C. Pomelli, J. W. Ochterski, R. L. Martin, K. Morokuma, V. G. Zakrzewski, G. A. Voth, P. Salvador, J. J. Dannenberg, S. Dapprich, A. D. Daniels, O. Farkas, J. B. Foresman, J. V. Ortiz, J. Cioslowski, and D. J. Fox, Gaussian, Inc., Wallingford CT, **2013**.

(4) “M86-E01078 APEX2 User Manual”, Bruker AXS Inc., Madison, USA, 2006.

(5) Sheldrick, G. M. Phase annealing in *SHELX*-90: direct methods for larger structures *Acta Cryst.* **1990**, *A46*, 467-473.

(6) Sheldrick, G. M. A Short History of SHELX. *Acta Cryst.* **2008**, *A64*, 112-122.